



2018

SYNTHESIS OF SEISMIC MOTIONS IN VIEW OF SOURCE TO SITE :THE KOBE CASE

Hirokazu TAKEMIYA¹, Gen MIYAGAWA² And Yuji KAGAWA³

SUMMARY

The 3-dimensional seismic wave simulation in Kobe due to fault rupturing in the Hyogoken Nanbu Earthquake (1995) is performed. Based on the kinematic dislocation model, the ground motions are solved by the convolution scheme in time for source function and in space along rupture direction with the newly developed Green function for distributed loads. Focused are the effects of asperity in fault rupturing and the soil layering on the transient response. Inhomogeneous rupture mechanism is considered in terms of a multiple asperities. The synthetic motions based on the inversion information from the observed data are compared well with the KBU record on soft rock. Secondly, in view of the deep soil and shallow soil deposits at site, the seismic wave amplification is analyzed by the 2-DFEM-BEM method and by the 1-D analysis, respectively. The modification of the ground motions that resemble the KBU record is interpreted from wave interference. Compatible amplification is observed along the horizontal distance with that from the observed data. The response spectrum computed proved the surface soft layer effect of amplification in the lower period range than 1 second, attaining compatible values for the JMA record on alluvium.

INTRODUCTION

The Hyogoken Nanbu Earthquake, 1995 (M=7.2), was the most devastating inland type earthquake that Japan has ever experienced. In the heaviest damage zone it was registered as the intensity 7 (severest) on the Japan Meteorological Agency (JMA) scale [3]. It stretched out in a narrow band along the fault line but was offset with some short distance, roughly 1 km, from the fault line [3]. During the main shock, the earthquake motions were recorded at several locations. The records at the Kobe Marine Meteorological Observatory (JMA-Kobe) on alluvium and at the Kobe University basement (KBU) on soft rock were the representatives whose characteristics were the unexpectedly high velocity and large displacement in addition to the big acceleration with unusual longer predominant periods than 1 second. The shallow and deep layered geology and their irregular boundaries in Kobe (see Fig.1 [6]), besides the unique fault rupture mechanism at the source, supposedly caused these observation results.

In case of shallow source earthquakes, the near surface geology apparently comes into effect substantially in the ground motions generated. After earthquake events, seismologists, based on source model available, detect the source parameters inversely from observed motions. Even from thus obtained limited information, we attempt the forward analysis for predicting the ground motions. Recently, for predicting ground motions due to big earthquakes, the use of small earthquake records at focused site is attractive as the Green function that fulfill not only the fault mechanism but also the geological conditions [2]. However, this imperial approach can seldom be expected practical unless dense array observation has long been continued. Therefore, some reliable analytical prediction methods should be developed. With additional some appropriate assumptions on the source

¹ Department of Environmental and Civil Engineering, Okayama University, Japan Email: e_quakes@cc.okayama-u.ac.jp

² Graduate student Department of Environmental and Civil Engineering, Okayama University, Japan

³ Graduate student Department of Environmental and Civil Engineering, Okayama University, Japan

mechanism, we may improve the fitting of the synthetic motions with the observation and give the reliable prediction at other locations. The causality condition governs the transient response for multiple-segment rupture, in particular. We pay attention to the path through which seismic waves propagate. This path effect is caused mainly by the soil layering. Finally, the ground surface motions are affected significantly by the topography and geology at site. We may take two-step procedure to evaluate the seismic wave amplification by the deep soils and shallow soils separately. The former is considered by the 2-dimensional wave field while the latter is by the 1-dimensional wave propagation. In what follow, the Kobe motions in the Hyogoken Nanbu Earthquake are targeted for simulation.

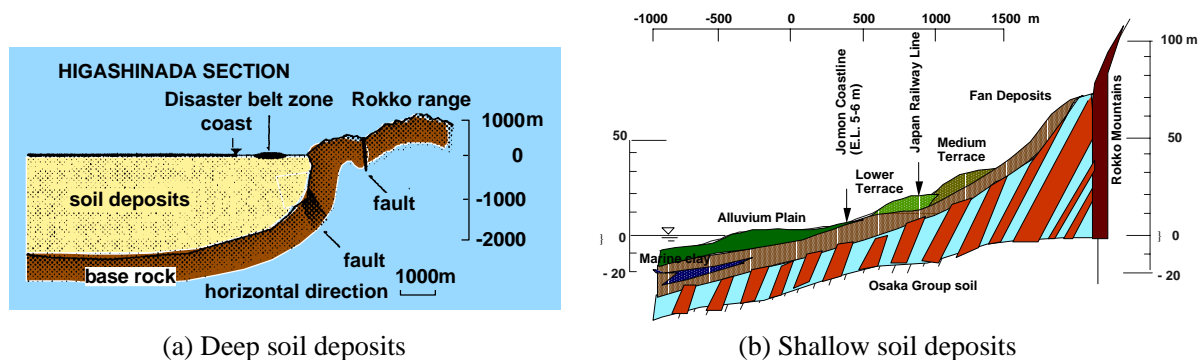


Fig.1 Typical geological structure in the Kobe area.

SYNTHETIC MOTIONS FROM KINEMATIC DISLOCATION

(1) Simulation system

The authors have developed a 3-dimensional simulation system of near-source motions with due account of kinematic fault rupture mechanism (dislocation theory). The solution method for the related moving Green function is to apply the Laplace-Fourier transforms respectively for time and space. The thin layer discretization is conveniently incorporated for the solution procedure in order to accommodate the geological layering. The double time convolution integral was implemented for the rupture process as characterized by the slip function and space propagation. The inverse Laplace transform is performed analytically and the inverse Fourier transform is carried out numerically when replaced by the discrete wave number method. The details are described in the authors publication [9, 10].

Some numerical procedures are interpreted as follows:

- 1) The kinematics of the fault dislocation is considered by the equivalent force action on fault area. The vertical discretization is predetermined by the thin layer procedure and the horizontal discretization follows the rupture speed and the time increment for analysis.
- 2) The rupture progress is controlled either by a unilateral Haskell model [1] or by a radial proceeding model of a constant slip rate or Kostrov type slip rate [5] that takes account of the stress drops after fault slip.
- 3) Since the solution method is based on the step-by-step integration of the convolution integral of the moving Green function for the equivalent dislocation force action, the time increment should duly be chosen in view of the frequency contents in generated motions.
- 4) In adopting discrete wave number method the fundamental wave length should therefore be predetermined according to the frequency contents considered.
- 5) The simulation accuracy has already been checked with the observed records at other shallow source earthquakes [11].

Of interest here is the wave fields in less stiff layers overlying stiffer bottom soil that includes the fault asperities whose rupture velocities may exceed that of the wave propagation in the former. More importantly, the causality effect of rupture of multiple asperities is focused.

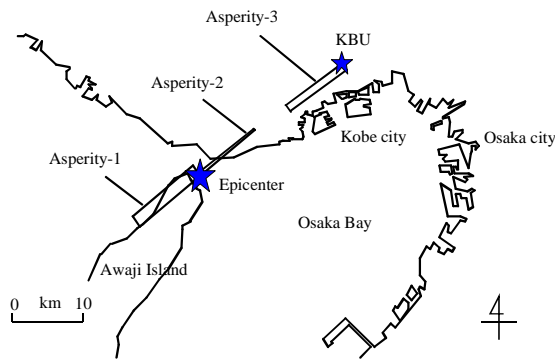


Fig.2 Plan view of the fault segments in the Hyogoken Nanbu Earthquake (1995)

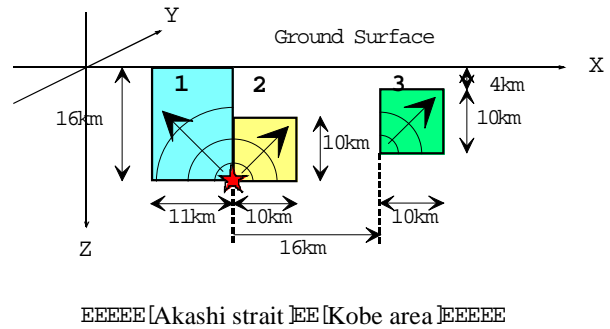


Fig.3 Fault segments for the Hyogoken Nanbu Earthquake (1995)

(2) Simulation Results

Figs.2 and 3 depict the fault area comprising three asperities that caused the Hyogoken Nanbu earthquake. The present study is first to targeted to simulate the Kobe University (KBU) record, representing the motions on rock very close to the fault line. Following the source information available from the inversion analysis[4], the updated three fault asperities in **Table 1** are employed. The location of the No.1 asperity is assumed to start rupturing from the Northeast lower corner and to proceed toward the Awajishima Island, the No.2 asperity from the Southwest lower corner and toward Kobe City, and the No. 3 from the Southwest lower corner and toward Kobe University. The Kobe University is located on the Southeast side of the strike line of the No. 1 and No.2 asperities, and on the Northwest side of the strike line of the No.3 asperity. The site condition that includes the quantitative features of these asperities is given in **Table 2**. The discretized model for the numerical computation is explained in **Table 3**. The rupture progress is presumed to be a radial propagation with either a constant slip rate [1] or a simplified Kostrov type slip rate [11].

Table 1 Seismic parameters

Segment No.	Time(s)	Mo (10 ¹⁹ Nm)	M _w	strike, dip, rake(degree)	Area (km ²)	Slip (m)
1	0~72	1.00	Total 6.9	(233, 85,175)	11x16	1.6
2	0~5.0	0.34		(233, 110,30)	10x10	0.9
3	6.2~11.2	0.18		(233, 100,60)	10x10	0.5
Total	0~11.2	1.52				
Rupture Velocity(V _r) = 2.8 (km/sec) Rise Time = 0.6(sec)						

Table 2 Soil parameters

Layers No.	Thickness (km)	P wave velocity V _p (km/s)	S wave velocity V _s (km/s)	Poisson's ratio ν	Density ρ (x10 ⁹ t/km ²)
1	0.7	2.5	1.4	0.272	1.8
2	1.2	4.0	2.3	0.253	2.0
3	1.5	5.2	3.0	0.251	2.4
Bottom Layer	Infinite	6.0	3.5	0.242	2.8

Table 3 Parameters for numerical computation

Base Depth	Numbers of Sub-division	Fundamental wave length	Maximum Frequency	Maximum Wave Number	Time Step Numbers	Time increment
104.4 km	104	204.8 km	15 rad/s	4.6 rad/km	300	0.1 [s]

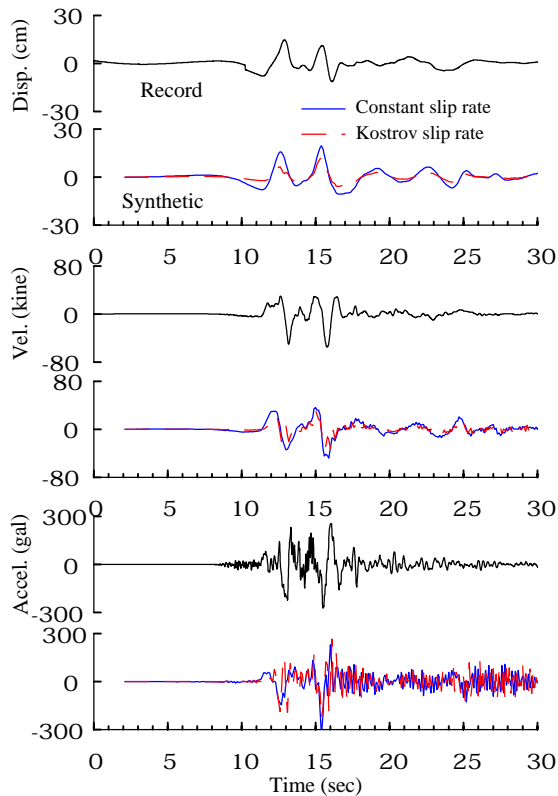


Fig.4.a Comparison of synthetic motions with recorded motions (NS component)

The computation results are filtered in order to extract only the essential response features. The trapezoidal filtering window is used for the final evaluation of displacement, velocity and acceleration responses, which specifies as 0.1 to 0.4 Hz for low frequencies' linear build up and as 23 to 25Hz for high frequencies linear die off. **Fig.4.a, b** and **c** are the resulting time histories for horizontal and vertical displacements, velocities and accelerations for different directional components. The difference between the types of the seismic slip functions is noted small. These synthetic motions are compared with the observed records. The matching is very good for the almost strike normal NS component in the displacement and velocity and acceleration in the major portion. The WE component is overestimated for the displacement and velocity while underestimated for the acceleration. The vertical component is underestimated significantly for all response quantities. These discrepancies however are improved in the succeeding analysis by taking into account of the site effects that came into the recordings through seismic wave propagation.

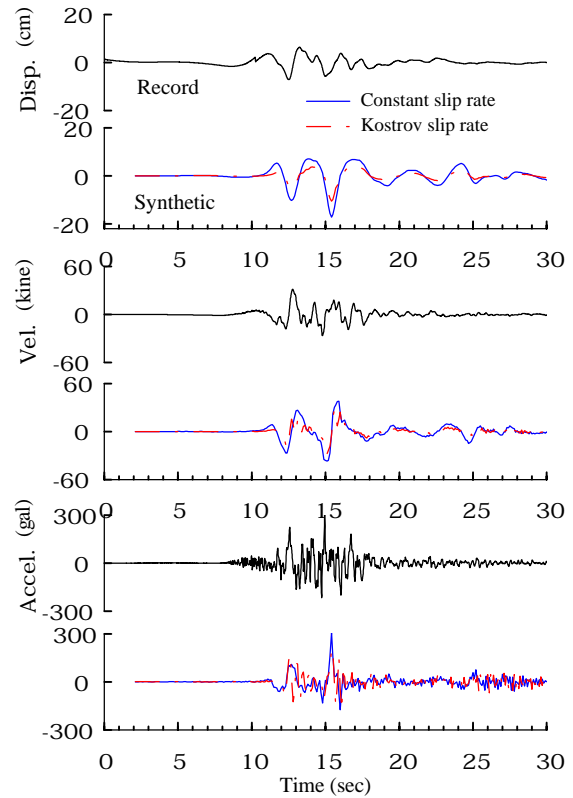


Fig.4.b Comparison of synthetic motions with recorded motions (EW component)

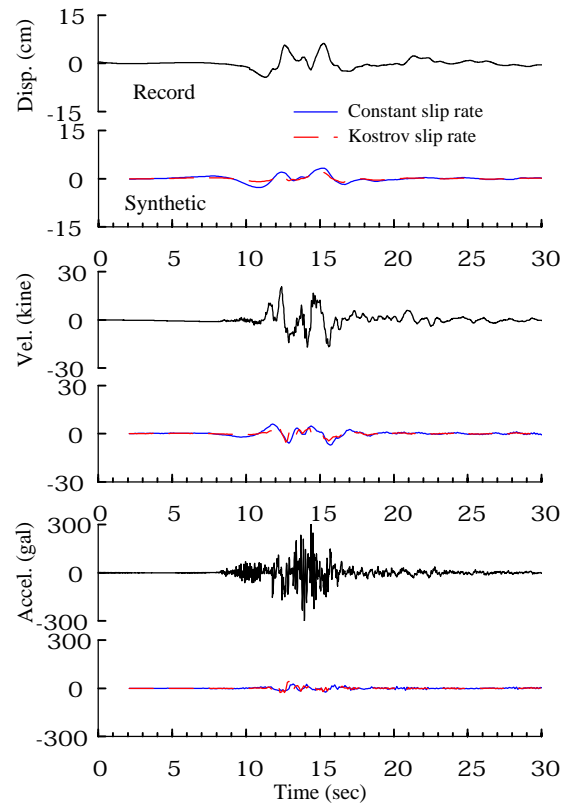


Fig.4.c Comparison of synthetic motions with recorded motions (UD component)

SITE EFFECTS FROM WAVE PROPAGATION IN DEEP/SHALLOW SOILS

The variation of ground motions along the north-south direction from the foot of Rokko ranges to the Seto Inland Seacoast is the main interest herein. In view of the topography and geology effects on seismic wave propagation, the deep stiff soil called Osaka group layers and the overlying soft alluvium are separately considered by taking respective models.

(1) Deep soil response

The computer simulation is conducted by employing the two dimensional time domain FEM-BEM hybrid technique [7,8]. The irregularly configured soil deposits are modeled by the finite elements while the surrounding halfspace is modeled by the compatible boundary. The discretization is made to fulfill the wave propagation of considered wavelengths. Only vertical wave incidence is assumed in what follows.

In view of the abrupt dipping of the rock formation at the foot of the Rokko range, the wave propagation is focused on the deep Osaka group layers overlying it. **Fig.5** shows the FEM-BEM model for the computer simulation. The dimensions of the model are assumed as shown in the figure by referring to the available related information [6], and the material properties are indicated in **Table 4**. The material damping is assigned to the finite element domain as small as 3% in the so-called Rayleigh damping factor. The horizontal as well as vertical components from the foregoing seismic motions from the fault rupture are used by assuming the horizontal and vertical simultaneous components as the S-wave and P-wave incidence, respectively..

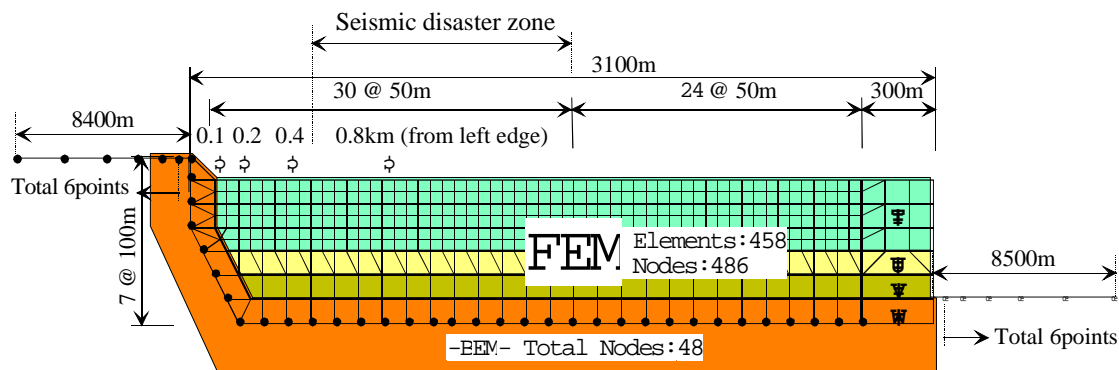


Fig.5 Deep soil model for FEM-BEM analysis

Table 4 Soil properties of deep soil model

Soil Zone	Shear wave velocity V_s (m/s)	Density ρ (t/m^3)	Poisson's ratio ν	Damping ratio h
FEM I	500	2.0	0.33	0.05
FEM II	800	2.2	0.30	0.02
FEM III	1000	2.2	0.30	0.02
FEM IV	2000	2.2	0.25	0.02
BEM	2000	2.2	0.25	—

Fig.6 is the response time histories at the specific surface location as indicated in **Fig.5** by the symbol ϕ . Only velocity and acceleration components are depicted since the former is investigated with respect to the frequency contents and the latter is used as input motions to the succeeding surface layer analysis. **Figs.7.a, b** and **c** show the maximum response profiles for displacement, velocity and acceleration, respectively for horizontal and vertical components. The amplifications differ according to the response quantities focused: the acceleration and velocity have their peak locations at specific distance from the edge of soil deposits. For the horizontal motions this location is about several hundred meters. However, for the vertical motions it is very close to the edge. Interesting to note is the higher vertical acceleration than the horizontal acceleration at this distance. This phenomenon was actually recognized at the KBU records. In order to investigate the amplified frequency contents, the Fourier amplitudes of velocity response are compared in **Fig.8(a)** for different horizontal distances from the edge. For the horizontal motion the frequency contents in the range of 0.3 ~ 0.4 Hz are predominant

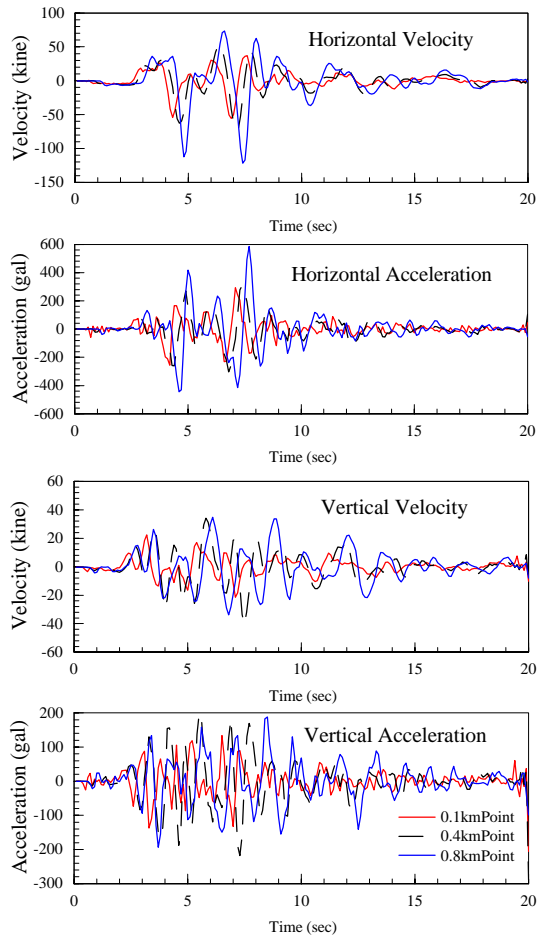


Fig.6 Response time histories from deep soil model

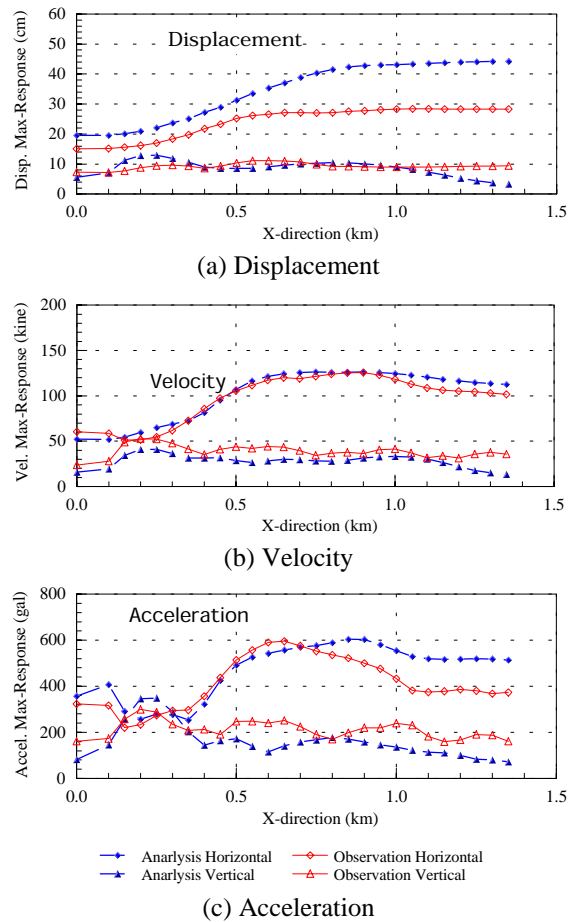
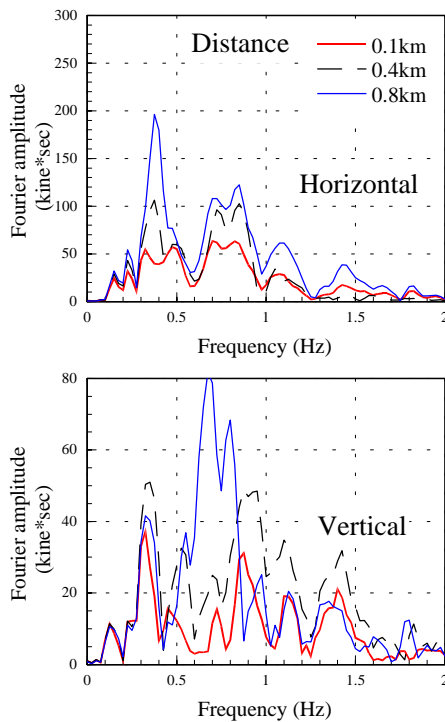
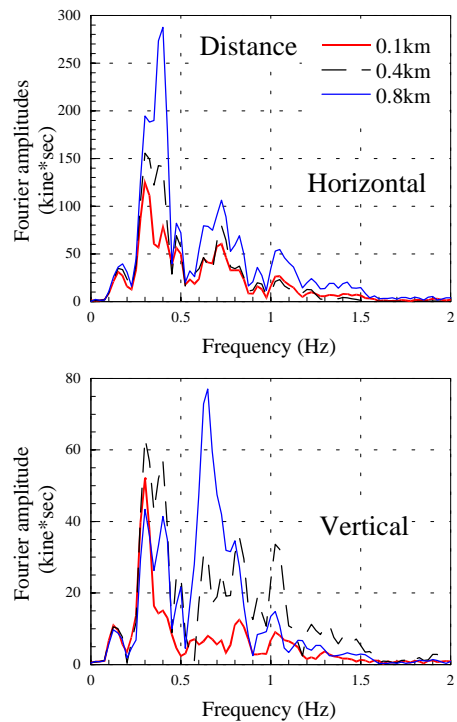


Fig.7 Maximum response profile at top of the base soil (Deep soil model)



(a) Due to KBU record as SV&P incidence



(b) Due to synthetic motions as SV&P incidence

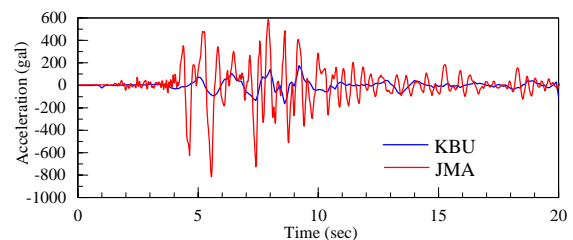
Fig.8 Fourier amplitudes of velocity responses at locations of various distances in deep soil model

while in the vertical motions the frequency contents in the range of 0.6 ~0.7 Hz becomes comparable. The peak frequencies are almost fixed for every focused location. In order to verify the present approach, the analysis was carried out for the KBU records. The results are shown in **Fig.8.(b)**. Those for the synthetic motions from the deep soil model are compared well with those for the KBU records. However, the former is more characterized by the dominant low frequency components below 0.5 Hz. This fact means that the dislocation effect still remains strongly in the wave field of deep soils..

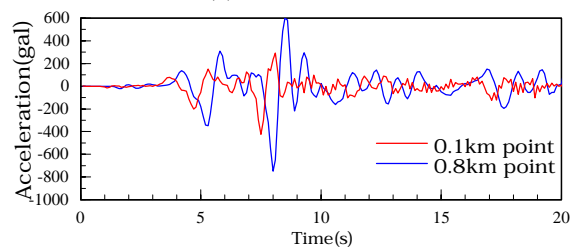
(2) Shallow soil effect

In order to interpret the amplification due to the shallow soil deposits, simply the one-dimensional shear wave field is presumed for evaluating the response amplification. As far as the maximum surface response values are concerned, this solution procedure may be acceptable. The authors' previous analysis [8] revealed that the soil deposits of 20m depth attained the equivalent viscous damping ratio as large as 20 %, while the soil deposits of 10 m depth as small as 3 %. Following this information, the responses are computed in **Fig.9** for those amplified surface motions additionally by the shallow soil deposits due to the input motions at the indicated distances from the deep soil model. Depending on the soil depth, the surface motions appear significantly different as being affected by the one-fourth wavelength resonance of the shear wave.

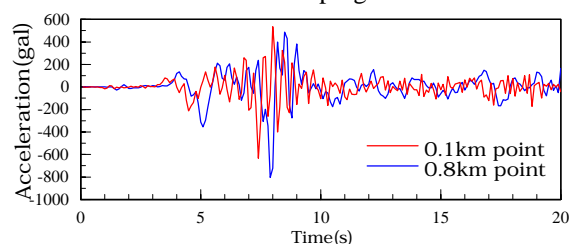
The response spectra are also computed for those amplified surface motions and shown in **Fig.10**. Note that an excellent matching of the response spectra at the distance 0.1 km for synthetic motion with that of the KBU, which means the successful simulation for the base motion. The difference of the values for the JMA and KBU records appears in the low period range less than 1 second and almost no difference beyond it. As the distance is increased in the deep soil model, the response spectra value is increased. The amplification is rather spread out in the low period range less than 1 second, attaining almost the same values for the JMA record. Also above 3 second the higher values results than that of JMA. This may be caused by the first low frequency predominant peak in the synthetic motion. The former amplification is due mainly to the surface shallow soil deposits while latter amplification is due mainly to the dislocation mechanism. However, the KBU and JMA do not have such a long period or the corresponding low frequency accuracy. This fact explains no amplification of this period range, though.



(a) Observation



(b) Simulation, Shallow soil of 20m depth, 20% damping



(c) Simulation, Shallow soil of 10m depth, 3% damping

Fig.9 Acceleration time histories additionally amplified by surface soils (1-D analysis)

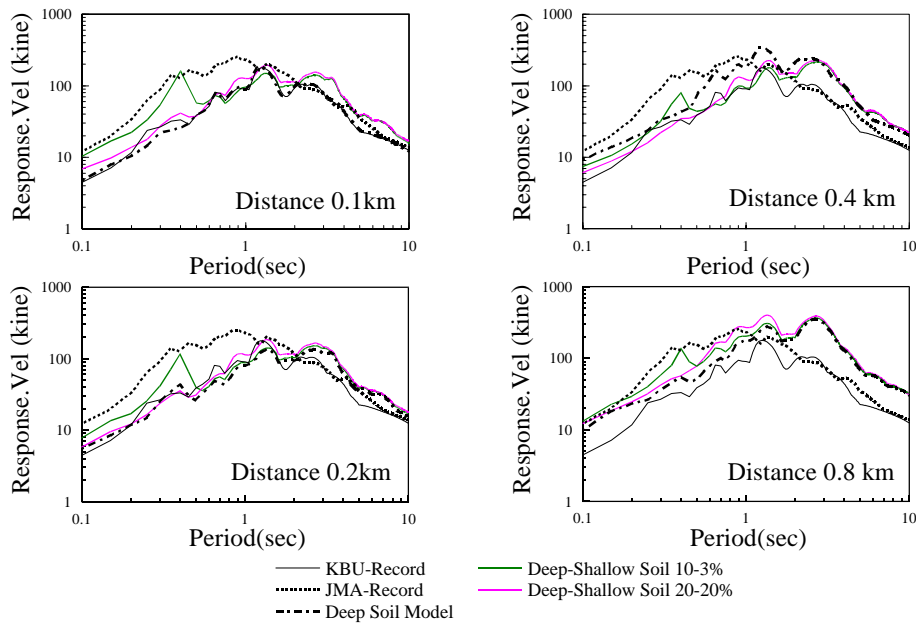


Fig.10 Response spectra (5% damping ratio)

CONCLUSIONS

1. Step-by-step solution procedures from dislocation, deep and shallow soil analyses resulted in a reasonable response spectra prediction for sever fault rupture earthquakes that lead the so-called L2 level structural design.
2. Regarding the seismic wave generation by multiple faults rupture, the case of the Hyogoken Nanbu Earthquake (1995) was simulated. Some acceptable computation results have been demonstrated for the targeted KBU record in terms of displacement and velocity components for the horizontal directions but not for the horizontal acceleration and for the vertical components.that includes higher frequencies than the former
3. The 2-dimensional simulation for the wave field has been conducted in view of the deep soil deposits in Kobe. The modification of the seismic wave field resulted in an improved comparison for the vertical component with the KBU record. The response spectrum indicated an excellent matching between for the KBU and for the present simulation.
4. The 1-dimensional wave field is computed in order to interpret the surface soft layer amplification. This effect shifted up the response spectral values in the lower period range below 1 second, leading a good matching with that for the JMA record.

REFERENCES

1. Haskell, N.A. (1964), Radiation pattern of surface waves from point sources in a multi-layered medium, *Bull.Seism. Soc. Am.*, 54, 377-394.
2. Irikura, K.(1983), Semi-empirical estimation of strong ground motions during large earthquakes, *Bull. Disas. Prev. Res. Inst. Kyoto Univ.* 33, 63-104.
3. Japan Society of Civil Engineers(1995), Report on the Great Hanshin Earthquake Disaster.
4. Kamae, K. and Irikura, K. (1997), "A fault model of the 1995Hygo-ken Nanbu Earthquake and simulation of strong ground motion in near-source area", *J. struc. Constr. Eng. Architectural Institute of Japan*, 500, 29-36.
5. Kostrov, B.V. (1964), "Self-similar problem of propagation of shear cracks", *J. appl. Math.* 28, 1077-1087.
6. Kobe City Office(1982), Kobe no Jiban (Ground of Kobe).
7. Takemiya, H. and Adam, M. (1997), "Seismic wave amplification due to topography and geology in Kobe during Hyogo-ken Nanbu Earthquake", *Structural Eng./Earthquake Eng. Japan Society of Civil Engineers*, 14, 2, 129s-138s. .
8. Takemiya, H. and Adam, M. (1998), 2D nonlinear seismic ground analysis by FEM-BEM: The case of Kobe in the Hyogo-ken Nanbu Earthquake, *Structural Eng./Earthquake Eng. Japan Society of Civil Engineers*, 15, 1, 19s-27s. .
9. Takemiya, H. and Goda, K. and Miyagawa, G. (1998), Simulation of near source ground motions due to multiple dislocations in layered soil, *The effect of Surface Geology on Seismic Motions*, 915-922.
10. Takemiya, H. and Goda, K. (1999), "Simulation of near source ground motions due to discretized dislocations in layered soil", to appear in the *Procs. Japan Society of Civil Engineers*.
11. Takemiya, H. and Miyagawa, G. (1999), "Simulation of near source ground motions due to dislocations in layered soils", Submitted to *Procs. Japan Society of Civil Engineers*.